THE ABLE-5 LUNAR SATELLITE

P. F. Glaser
E. R. Spangler

1. INTRODUCTION

The Able-5 lunar satellite (Figure 1) is the largest and the most sophisticated of the NASA/USAF Able series of space probes. It measures nearly nine feet from paddle tip to paddle tip and approximately five feet from the forward to the aft antennas. Its weight, 390 pounds, includes 115 pounds of instrumentation. This instrumentation constitutes an integrated system whose design has profited from the experience gained from the previous Able space probes, notably Explorer VI and Pioneer V.

Like the previous Able vehicles, Able-5 makes use of the three-stage launch vehicle, but with three important differences. First, the use of an Atlas ICBM as first stage, instead of a Thor IRBM, permits a heavier and larger payload than has previously been possible. Secondly, an advanced guidance system permits more precise control over the second stage than has heretofore been possible. Third, a multiple-start, monopropellant engine in the fourth stage, with fore and aft nozzles and variable burning times, permits flexible midcourse and terminal control of the satellite itself.

During launch the satellite sits with paddles folded down and attached to an interstage structure mounted atop the third stage. This third-fourth stage combination, enclosed in its fairing, is mated to the second stage, which in turn uses an interstage structure to mate to the Atlas (Figure 2).

The Able-5 lunar satellite operates, of course, as a single entity, and every detail of its configuration is closely connected to the operation of every other detail. For exposition, however, the satellite can be divided conveniently into four areas: the scientific experiments, the instrumentation, the engine, and the temperature control system. These four areas are discussed in some detail in the following sections.

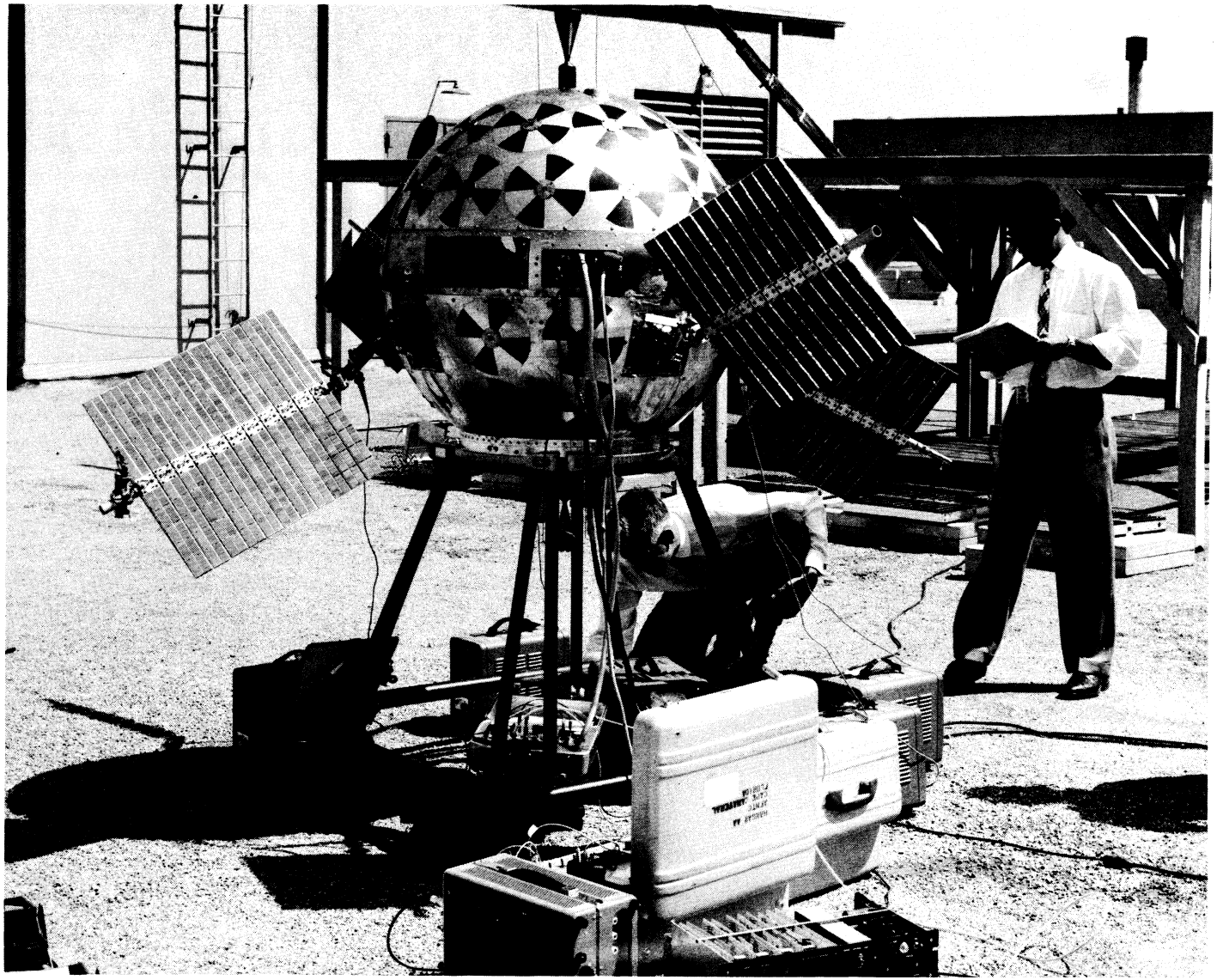

Figure 1. Able-5 Satellite During Final Checkout.

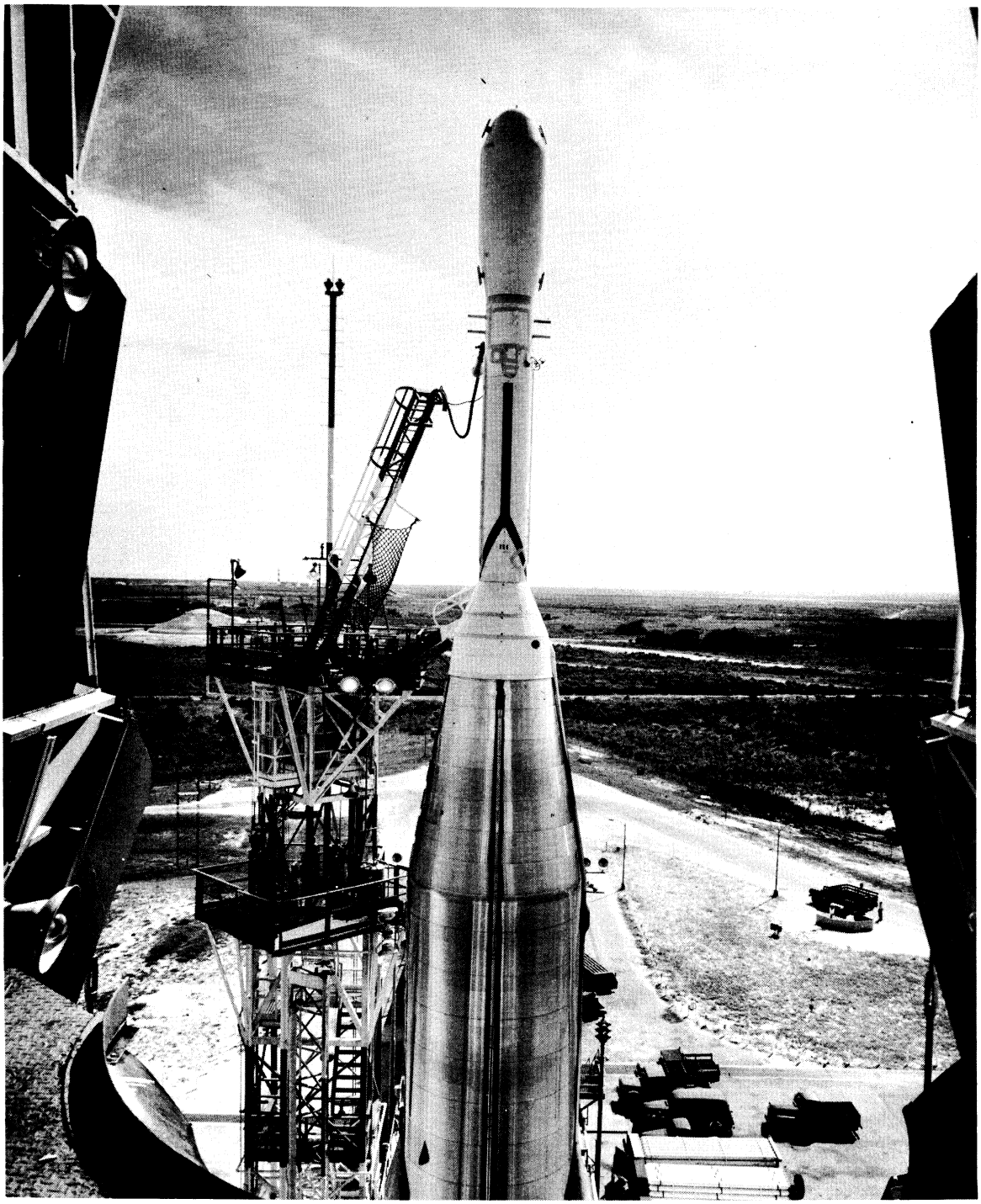

Figure 2. Top Stages of Able-5 Vehicle.

2. EXPERIMENTS

The principal goal of the Able-5 program in placing a scientific observatory in a relatively close (nominal perilune 1400 miles, apolune 2500 miles above the surface of the moon) lunar orbit is to provide scientific data concerning the moon, its immediate environment, and the space between the earth and the moon. The equipment carried aboard permits nine sets of experimental measurements to be made. These are listed in Table 1, together with their weights and power requirements. The location of most of the equipment used for these experiments can be seen in Figure 3.

Table 1. Able-5 Experiments.

Experiment	Weight (lb)	Power Requirement (mw)
Cosmic ray telescope	5.0	240
Scintillation spectrometer	3.35	309
Ion chamber and Geiger-Mueller tube	2.0	90
Low-energy scintillometer	2.25	340
Spin-coil magnetometer and phase comparator	2.0	220
Flux-gate magnetometer	2.1	192
Plasma probe	1.5	138
Micrometeorite detector	1.5	87
Space environment effects	0.5	20
Total	20.2	1636

2.1 Radiation

Because of the problems in the area of particle radiation in space that have been raised by previous space probes and because of the ability of radiation detectors to provide data broadly applicable to a variety of questions

1. COSMIC RAY TELESCOPE
2. PLASMA PROBE
3. TELEMETRY SIGNAL CONDITIONER
4. PHASE COMPARISON ANALYZER & SPIN COIL
5 DIGITAL TELEMETRY UNIT
6 MICROMETEORITE DIAPHRAGM
7 BATTERY PACK, 1-2
8 LOW ENERGY SCINTILLATION LOGIC
9 SCINTILLATION SPECTROMETER LOGIC
10 MATERIAL COATING PROBES
11 ANGULAR ACCELEROMETER
12 SCINTILLATION SPECTROMETER SENSOR
13 NO. 1 CONVERTER (EXPERIMENT SUPPLY)
14 LOW ENERGY SCINTILLATION COUNTER
15 FLUX GATE MAGNOTOMETER LOGIC AND AMPLIFIER
16 DIGITAL DECODER
17 MICROMETEORITE DIAPHRAGM
18 MICROMETEORITE AMPLIFIER
19 MICROMETEORITE SCALER

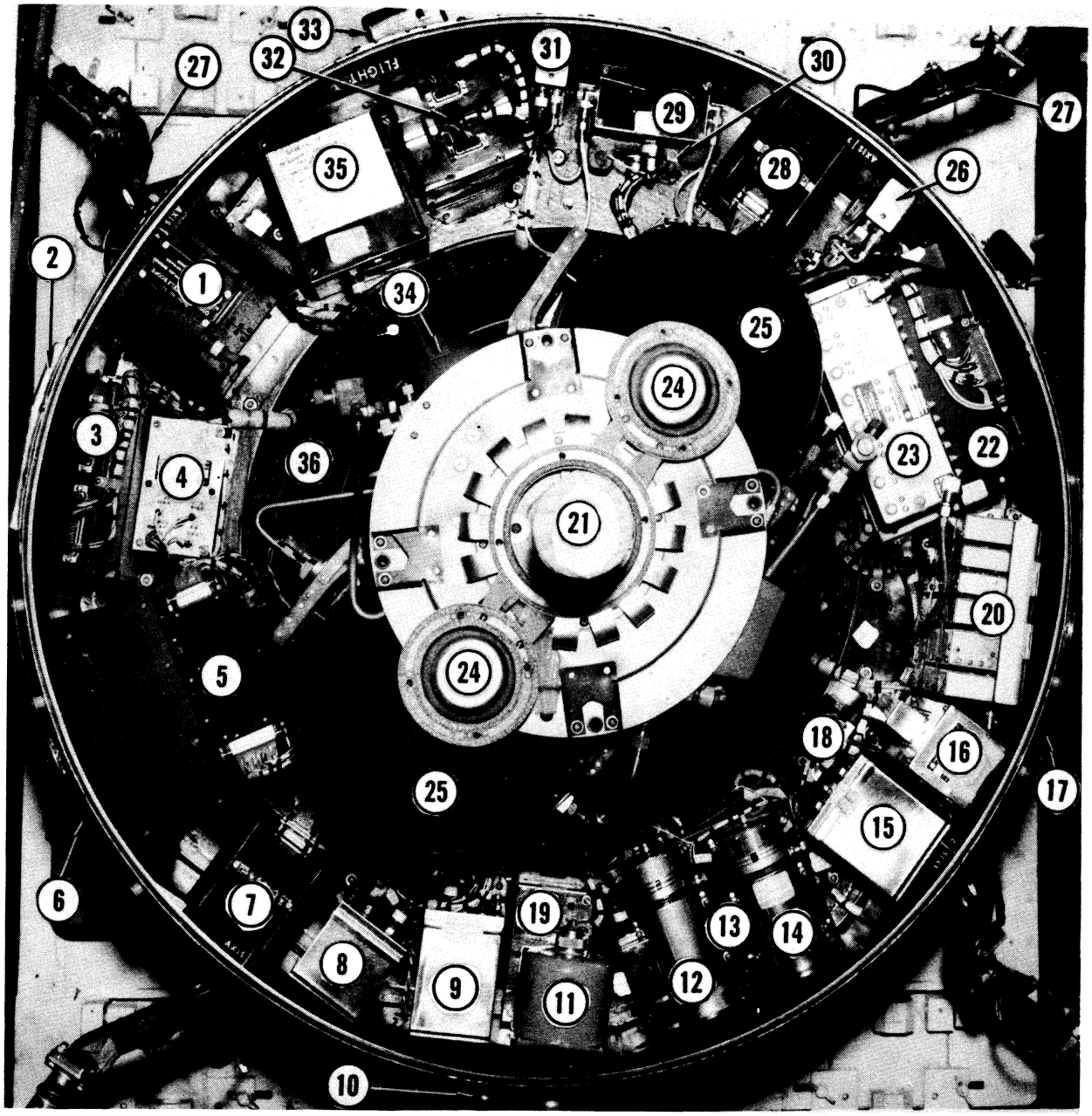

21 INJECTION THRUST CHAMBER
22 POWER DISTRIBUTION BOX
23 DIPLEXER
24 ANTENNAS
25 NITROGEN TANKS (MAIN PRESSURIZING)
26 COHERENT MODULATOR
27 SOLAR CELL PADDLE ARMS
28 BATTERY PACK, 3-4
29 NON-COHERENT TRANSMITTER (TOP)
30 COHERENT TRANSMITTER (BOTTOM)
31 NON-COHERENT MODULATOR
32 COHERENT AND NON-COHERENT CONVERTERS
33 SUN SCANNER
34 AUXILIARY PRESSURIZATION NITROGEN TANK
35 ION CHAMBER, GEIGER-MUELLER COUNTER
36 HYDRAZINE TANK

Figure 3. Internal View of Able-5.

concerning the lunar environment, the largest share of experimental sensors on Able-5 is devoted to radiation measurements. These are so designed that together they will measure radiation in a broad energy spectrum, ranging in energy per particle from 200 electron volts up to greater than 75 Mev. See Table 2.

Table 2. Characteristics of Radiation Sensors.

Instrument	Cutoff Energy and Efficiency		
	Electrons	Protons	X Rays
Low-energy scintillometer crystal: C_6H_4:$(CH)_2$:C_6H_4	> 50 kev ~ 100%	> 450 kev ~100%	> 50 kev ~ 0.1%
Scintillation spectrometer crystal: CsI	> 350 kev ~ 100%	> 2 Mev ~100%	> 350 kev ~ 4%
Cosmic-ray telescope argon, 60% } 600-mm CH_4, 40% } pressure	> 13 Mev ~ 100%	> 75 Mev ~100%	Must be determined experimentally
Ionization chamber argon, 4960-mm pressure	> 2 Mev ~ 100%	> 16 Mev ~100%	Must be determined experimentally
Geiger counter neon and halogens, 20-mm pressure	> 2 Mev ~80%	> 16 Mev ~80%	> 250 kev, 0.09% increasing linearly with particle energy
Plasma probe		> 0.20 to 20 kev ~40%	

Radiation will be measured by five experiments: (1) the low-energy scintillometer prepared by STL, (2) the scintillation spectrometer prepared by STL and Goddard Space Flight Center, (3) a University of Chicago cosmic-ray telescope, (4) the University of Minnesota ion chamber and Geiger counter, and (5) the Ames Research Center plasma probe. The experiments are designed

to determine the relative abundance of the different species of charged particles and to indicate their energy distribution.

Low-Energy Scintillometer

The low-energy scintillometer, Figure 4, measures the total flux of electrons of energy greater than 50 kev and of protons of energy greater than 450 kev. The detector is an anthracene crystal whose light pulses are detected with a Dumont 6467 photomultiplier. The detector is shielded from the front by an aluminum cap, 1.35 gm/cm^2 thick, through which a hole, 0.11 inch in diameter, admits radiation. A corresponding window in the payload shell admits radiation to the detector. To decrease noise in the output, the scaling circuit is biased above the random noise of the photomultiplier tube.

The total unit, housed in two packages, consists of the scintillometer and its shield, the photomultiplier, an amplifier, a scale of 2^{16} counter, and a readout circuit. The readout is the sum of the outputs of the 5th, 9th, and 16th binaries. A block diagram of the scintillometer is shown in Figure 5.

Scintillation Spectrometer

A scintillation spectrometer developed jointly for Able-5 by the Goddard Space Flight Center and STL generates an energy spectrum of protons of energies greater than 2 Mev and electrons of energies greater than 350 kev. The unit, shown in block diagram in Figure 6, consists of an inorganic scintillator crystal of cesium iodide doped with plutonium, an RCA 6199 photomultiplier tube, collimater, combined high gain-low gain pulse amplifier, a pulse height analyzer, scaler storage, and pulse shapers.

The crystal in the sensor unit faces radially out from the payload through a two-inch window in the payload shell. An aperture stop opens on command from the ground, after transit through the terrestrial radiation zone, and increases the geometrical factor by 10^5. The bias level is changed by means of a signal from the digital telemetry unit and is telemetered to the ground. The output is scaled by 2^4 and 2^{10} at the 1 or 8 pps readout rates and 2^2 and 2^8 at the 64 pps readout rate.

Figure 4. The Low-Energy Scintillometer in Able-5.

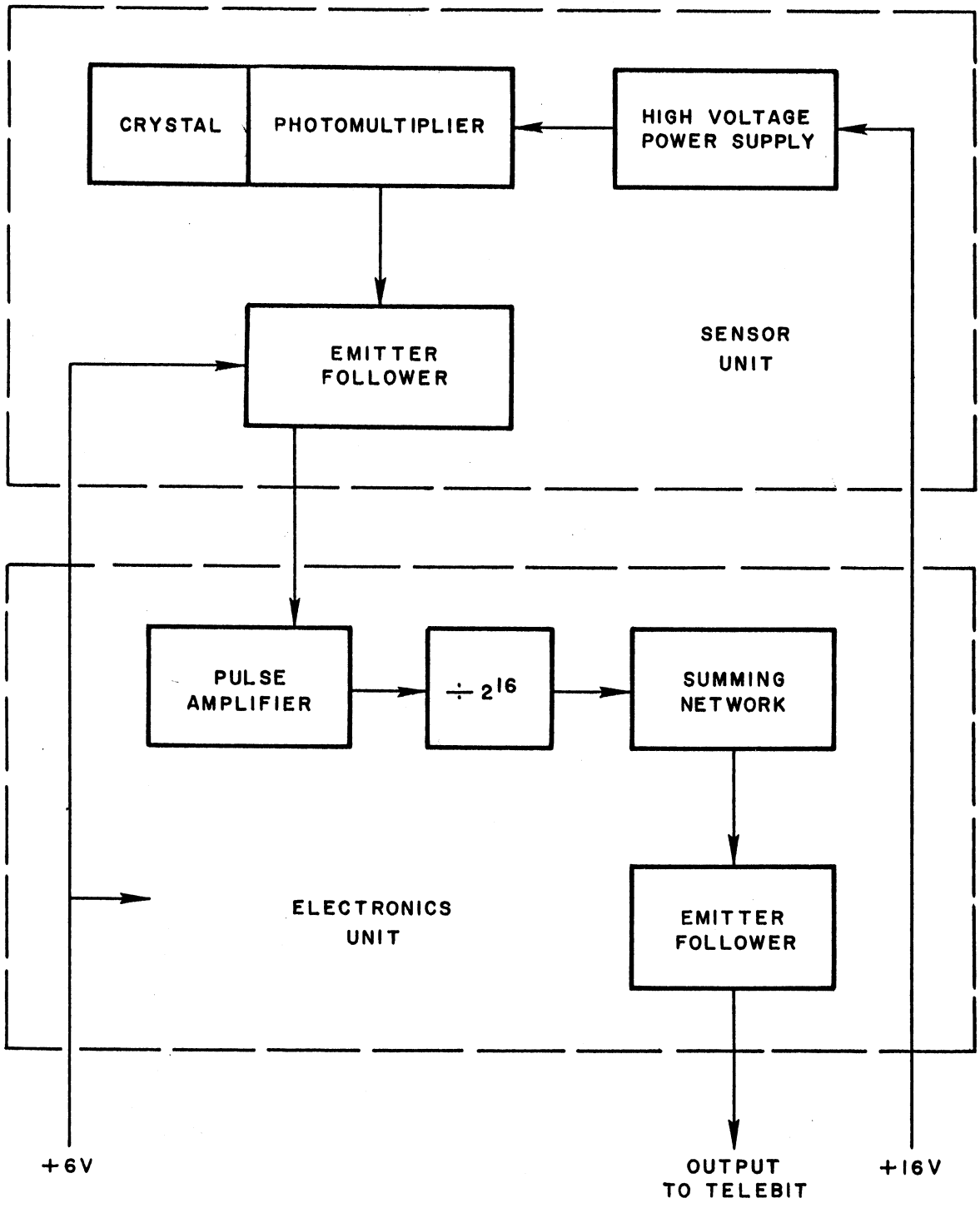

Figure 5. Block Diagram of Low-Energy Scintillation Counter.

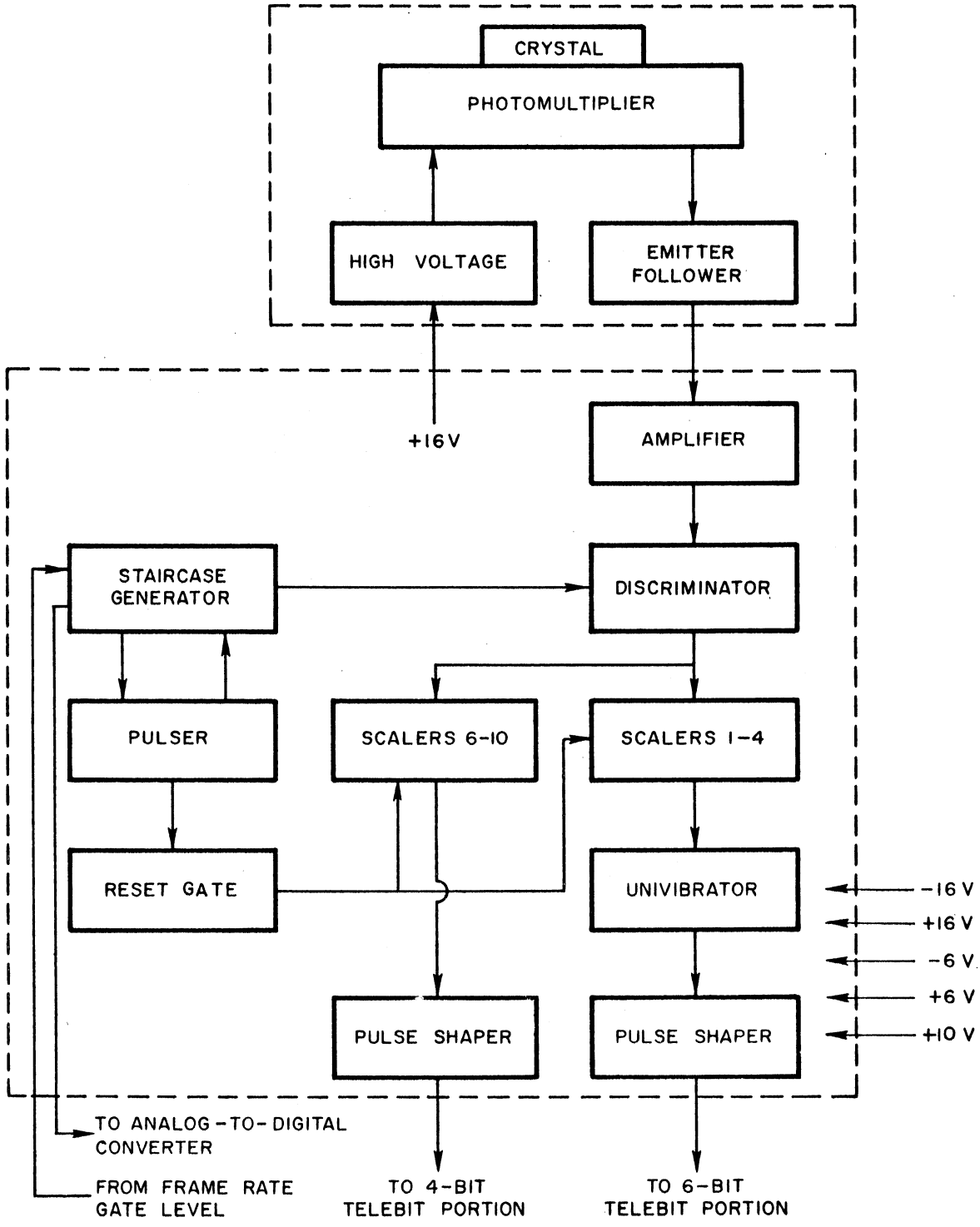

Figure 6. Block Diagram of Scintillation Spectrometer.

Cosmic-Ray Telescope

The cosmic-ray telescope, provided by the University of Chicago, contains a bundle of seven small proportional counters arranged in a configuration with a central counter surrounded by six outer counters. A cylindrical lead shield of 5 gm/cm^2 areal density encloses the counters. The counters are filled with a mixture of argon and methane to a pressure of about 600 millimeters. The center counter is connected to an amplifier with a threshold setting of about 1 millivolt; the amplifier operates a scaler chain of 2^9. Adjacent outside counters are connected together to form two groups of three. The output of each of the side groups is applied to a separate amplifier, which possesses 1-millivolt threshold. The output of all three amplifiers is used to activate a triple-coincidence circuit which drives a 2^9 scaler chain. (See Figure 7.)

The counter sensitivity is almost isotropic. A singles event corresponds to a charged particle traversing one outer counter and stopping in the central counter. Such an event triggers the 2^9 scaler chain. A triples event corresponds to a charged particle traversing one outer counter, the center counter, and stopping in or traversing a counter in the other group of three (i.e., the particle may pass through or be absorbed in the last counter). The single counter rate is also sensitive to secondary radiation formed in the vehicle.

The Ionization Chamber

The combination of ionization chamber and Geiger counter provided by the University of Minnesota measures the flux of electrons and protons. Both the flux of particles and the ionization produced by the particles are measured. The equipment, Figure 8, is mounted together in a housing measuring approximately $6 \times 4.5 \times 5.5$ inches.

The ionization chamber is of the integrating type used extensively on University of Minnesota balloon flights. It consists of a four-inch sphere filled with argon gas to an absolute pressure of approximately seven atmospheres. Ions are collected by a quartz rod, the upper end of which is coated with Aquadag. The conducting rod is charged to a positive potential of 225 volts by an 8-micron, gold-coated quartz fiber mounted on a side arm. When the fiber is connected to

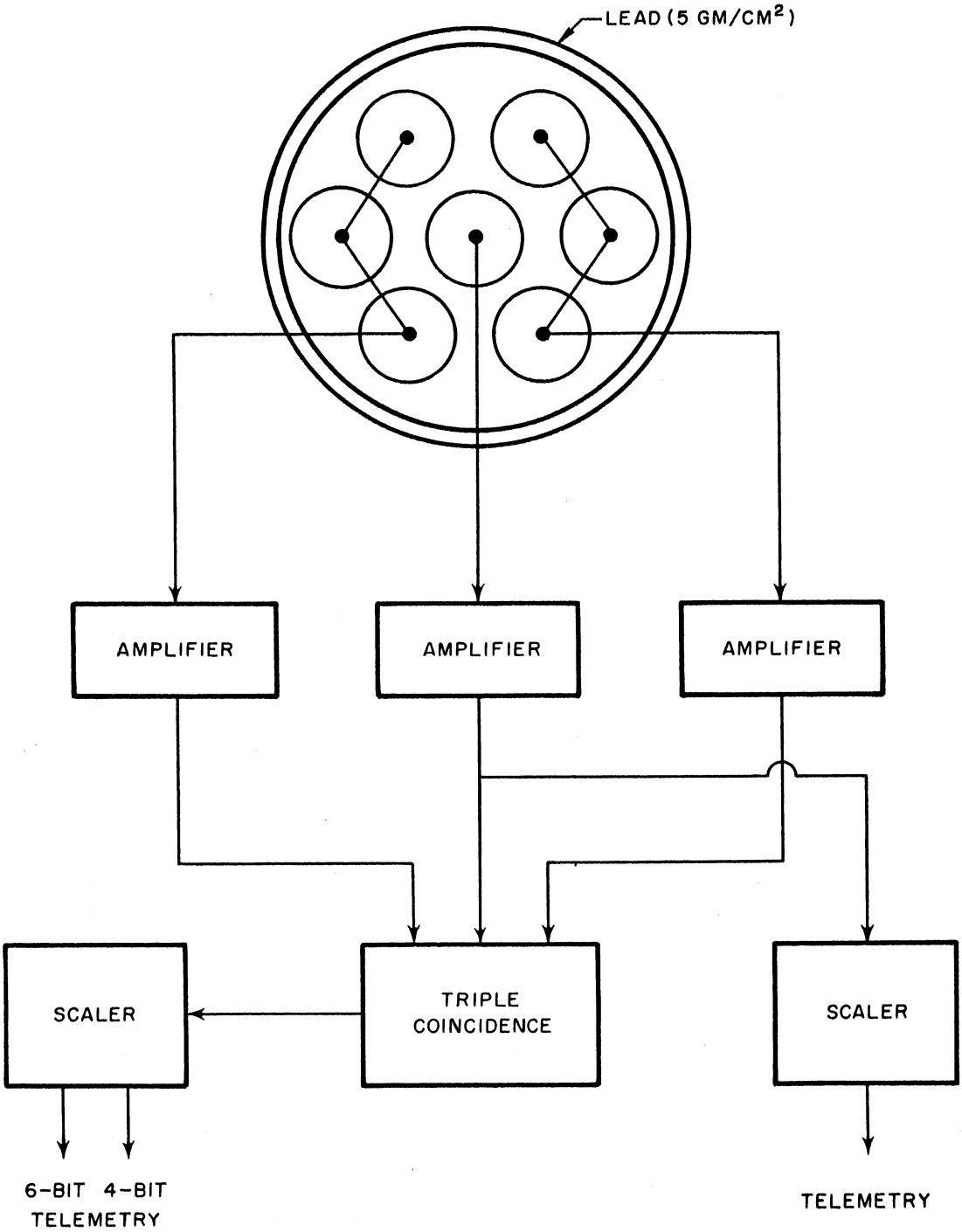

Figure 7. Block Diagram of Cosmic-Ray Telescope.

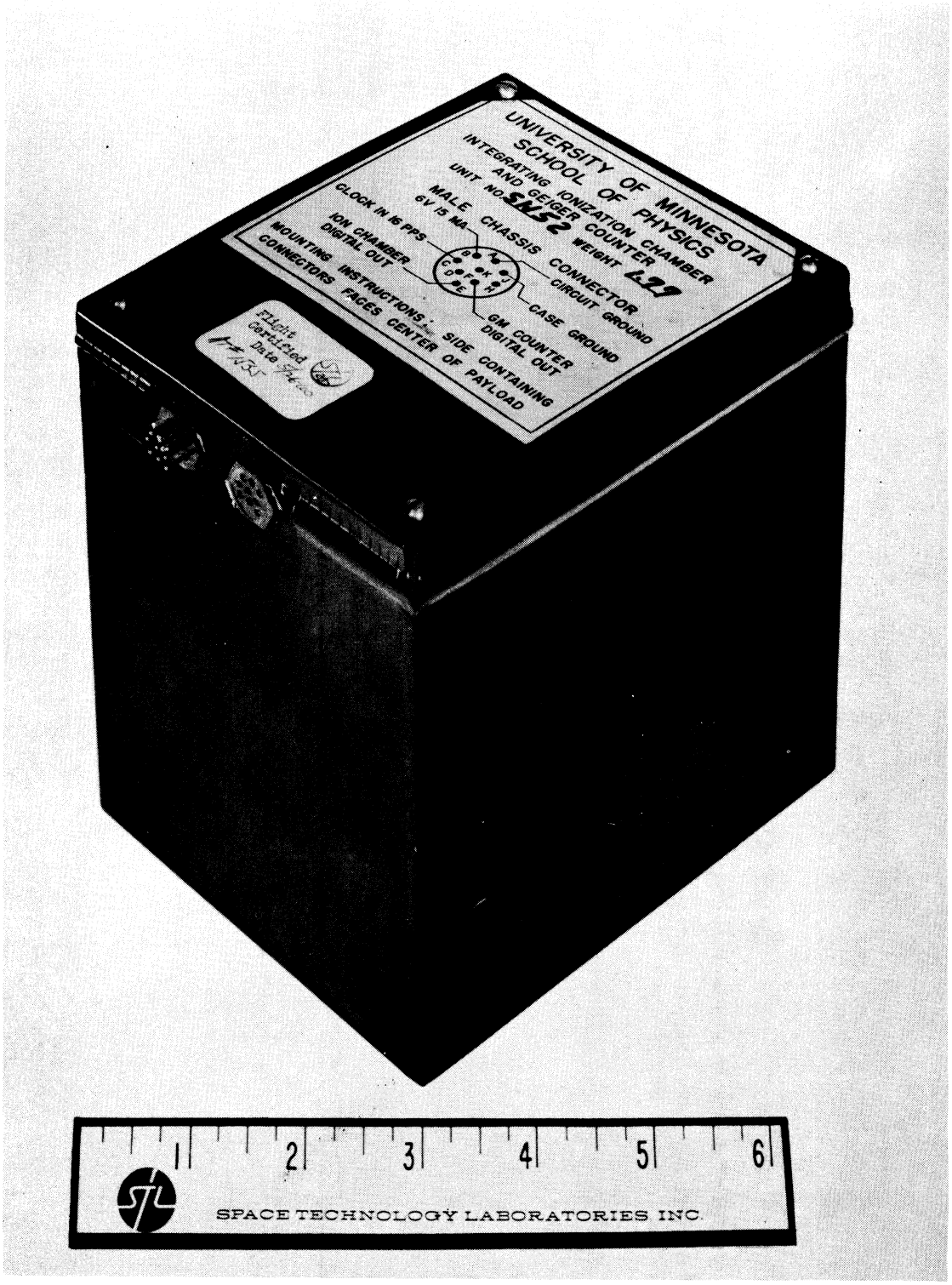

Figure 8. Ionization Chamber and Geiger-Mueller Tube Combination.

the positive potential, it is attracted to the rod, charging the system to the full potential of 225 volts. The fiber is then repelled by the electrostatic charge of the system. As the central rod collects electrons formed by ionizing radiation in the argon gas of the chamber, its potential drops and the fiber moves back until it is close enough to be attracted by the image charge. The fiber then recharges the rod and the charging pulse actuates the external circuit. Thus each pulse from the chamber represents the collection of approximately 2×10^{-10} coulomb of electricity.

The Geiger Counter

The second detector used by the University of Minnesota is a small Halogen Geiger Counter (Anton Type 302). The tube contains a mixture of neon and halogen gases to a pressure of approximately 20 mm of mercury. The data are processed in the same manner as the ion chamber and a scale factor of 2^9 is used.

Plasma Probe

The radiation sensor with the lowest energy threshold is the plasma probe provided by the Ames Research Center. (See Figure 9.) This equipment measures the flux of low-energy protons (0.2 to 20 kev) by means of a slit, an electrostatic analyzer, and an electrometer which collects the protons and develops a voltage across a high impedance proportional to the flux of protons. The analyzer consists of a pair of hemispherical concentric plates across which an electrical field varying from a few volts to 3000 volts is applied. For any given voltage the analyzer accepts protons which are approximately ±15 per cent of the energy of the proton which traverses the analyzer along a median trajectory. It becomes a necessity, therefore, to change the voltage across the plates successively in steps of approximately 15 per cent. Such a change is commanded by a pulse delivered by the telemetry unit and synchronized to the plasma probe experiment readout. The plasma probe exhibits a geometrical sensitivity of ±80 degrees measured from the normal to the slit in the long direction of the slit, and ±6 degrees measured from the normal and in the normal plane at right angles to the slit. Consequently, the plasma probe possesses a fan beam of sensitivity. As

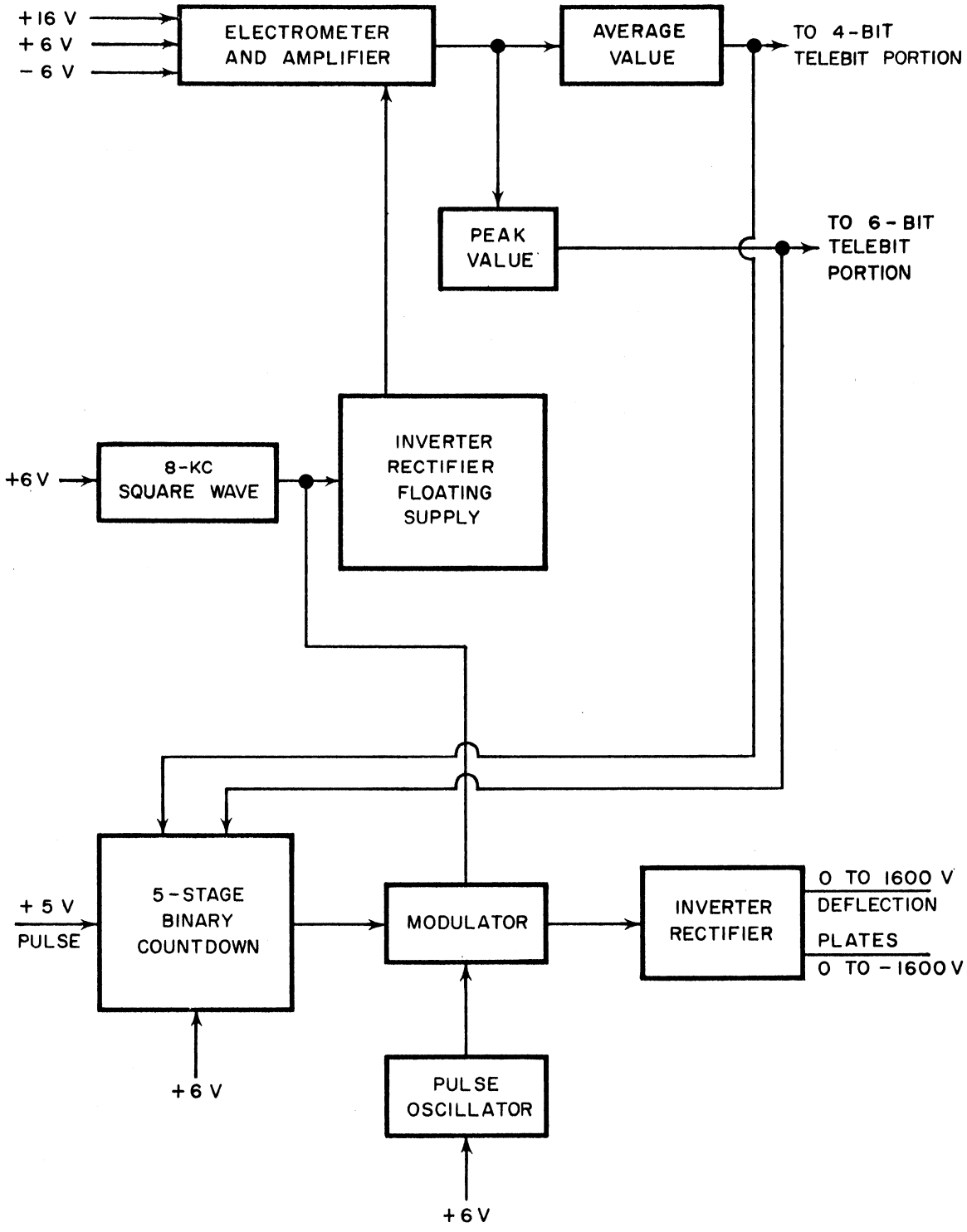

Figure 9. Ames Research Center Plasma Probe.

the payload spins the fan sweeps across about 95 per cent of the possible directions of arrival of protons impinging on the payload. The plasma probe generates signals which measure the peak and the average proton flux and delivers these signals to the digital telemetry unit.

2.2 Magnetic Field Measurements

The Search-Coil Magnetometer

The search-coil magnetometer provided by STL shows a sensitivity of approximately 0.3 gamma (3×10^{-6} gauss) for a steady field and about 2 gamma for varying fields. It consists of a mumetal core wound with 5000 turns of No. 40 copper wire. This coil is mounted on the end of a solar cell paddle spar in line with the longitudinal axis of the spar. The output of the coil is coupled to a transistorized amplifier tuned to the nominal spin rate of the vehicle. In a steady magnetic field the amplifier output is a sinusoid at a frequency equal to the spin rate. The magnetometer has a nonlinear transfer function which allows measurement of fields from less than 1 to about 1000 gamm. A block diagram of the unit is shown in Figure 10.

By making use of the 2.8-rps spin of the vehicle and knowledge of the orientation of the axis of this spin, the magnitude of the magnetic field and the direction of field can be deduced. A comparator which measures the phase relationship between the output of a photodiode sun scanner, or aspect indicator, and the output of the search-coil magnetometer provides the means by which to determine the direction of the field perpendicular to the spin axis. When data proportional to the flux-gate magnetometer output are related to the search coil output and the phase comparator information, the vector direction of the ambient field can be computed.

The Flux-Gate Magnetometer

The flux-gate magnetometer (Figure 11) consists of a probe, mounted along the longitudinal axis of the solar cell paddle spar, and the circuit chassis. The output voltage is a linear function of the field being measured. Three range scales can be designated by ground command: ±32 gamma, ±320 gamma, and ±3200 gamma. Also by command, a bucking current can be applied to effect discrete steps of

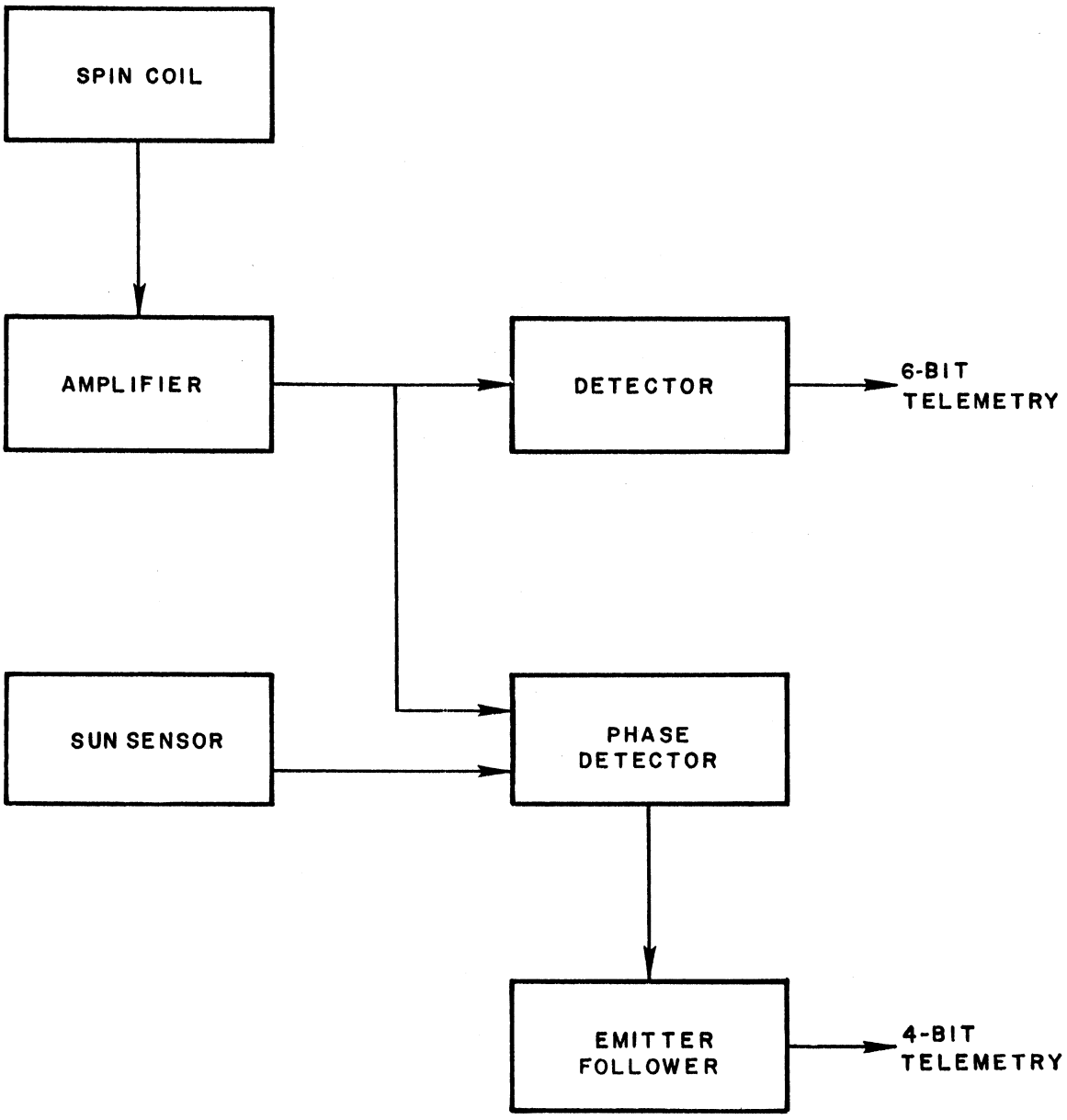

Figure 10. Block Diagram of Spin-Coil Magnetometer.

Figure 11. Flux-Gate Magnetometer.

40 gamma. In-flight calibration of the electronic system can also be made by ground command by shorting out the core secondary. The flux-gate magnetometer measures the ambient field parallel to the payload spin axis. Figure 12 shows a functional block diagram of the flux-gate unit.

2.3 Micrometeorite Detector

The micrometeorite experiment, sponsored jointly by the Goddard Space Flight Center and STL, measures the density and to an extent the energy spectrum of dust particles encountered in space. Impacts are detected with microphones located on two plates on the outer payload shell (see Figure 13). Impulses equivalent to two ranges of momenta are electronically selected by counting impulses after different degrees of amplification and discriminating against certain pulse amplitudes. By such implementation, two ranges of pulses are selected representing momenta greater than about 10^{-4} gm cm/sec (called (A) impulses in Figure 14) and momenta greater than 3×10^{-3} gm cm/sec (called (B) impulses). The microphones and amplifiers are supplied by Goddard Space Flight Center, the diaphragm and scalers by STL.

2.4 Space Environment Effects

Three spheres mounted on the surface of the payload near the equator are carried to measure the effects of the space environment on the thermal properties of three types of coating material. These are discussed further in Section 5.

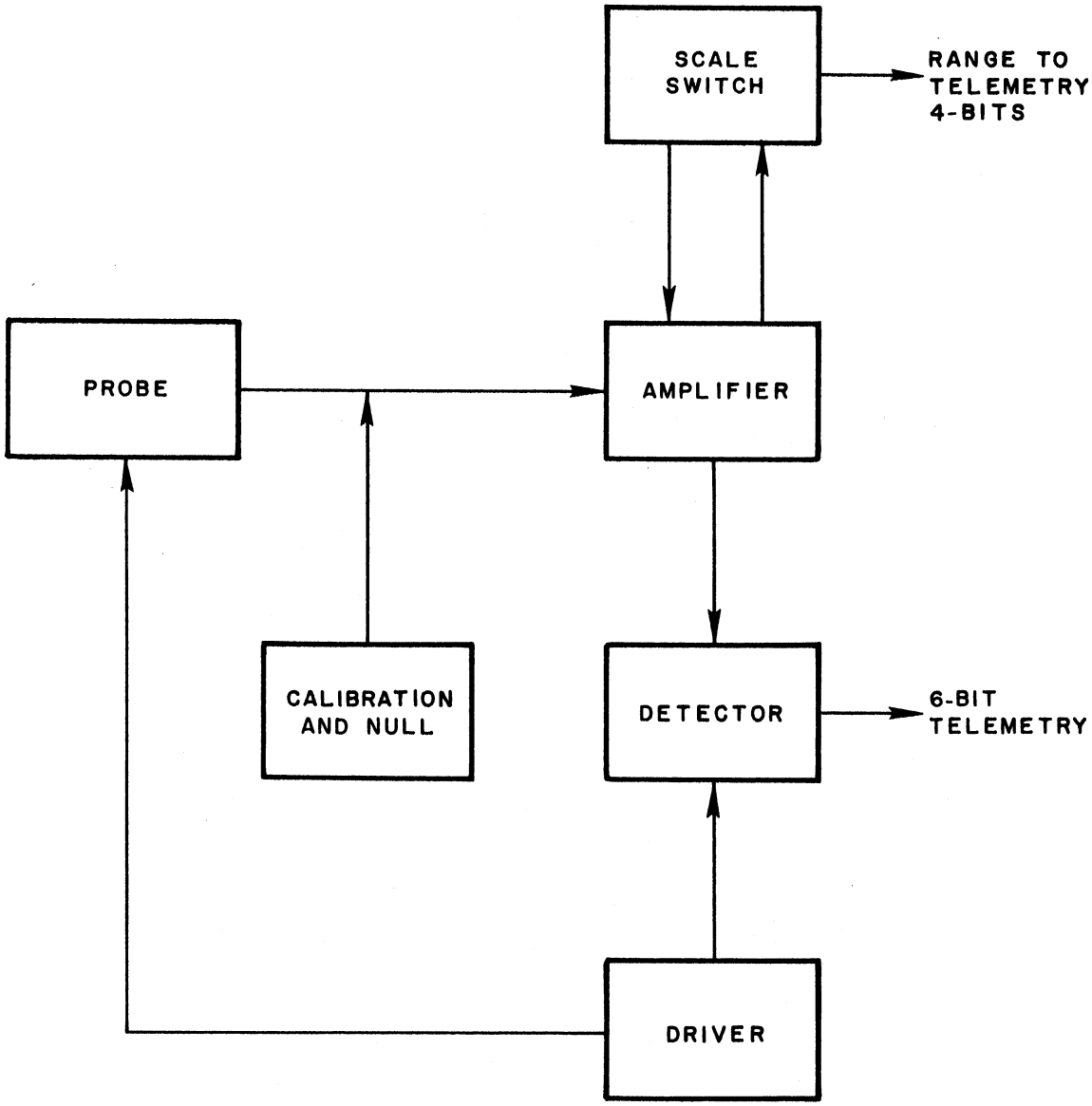

Figure 12. Block Diagram of Flux-Gate Magnetometer.

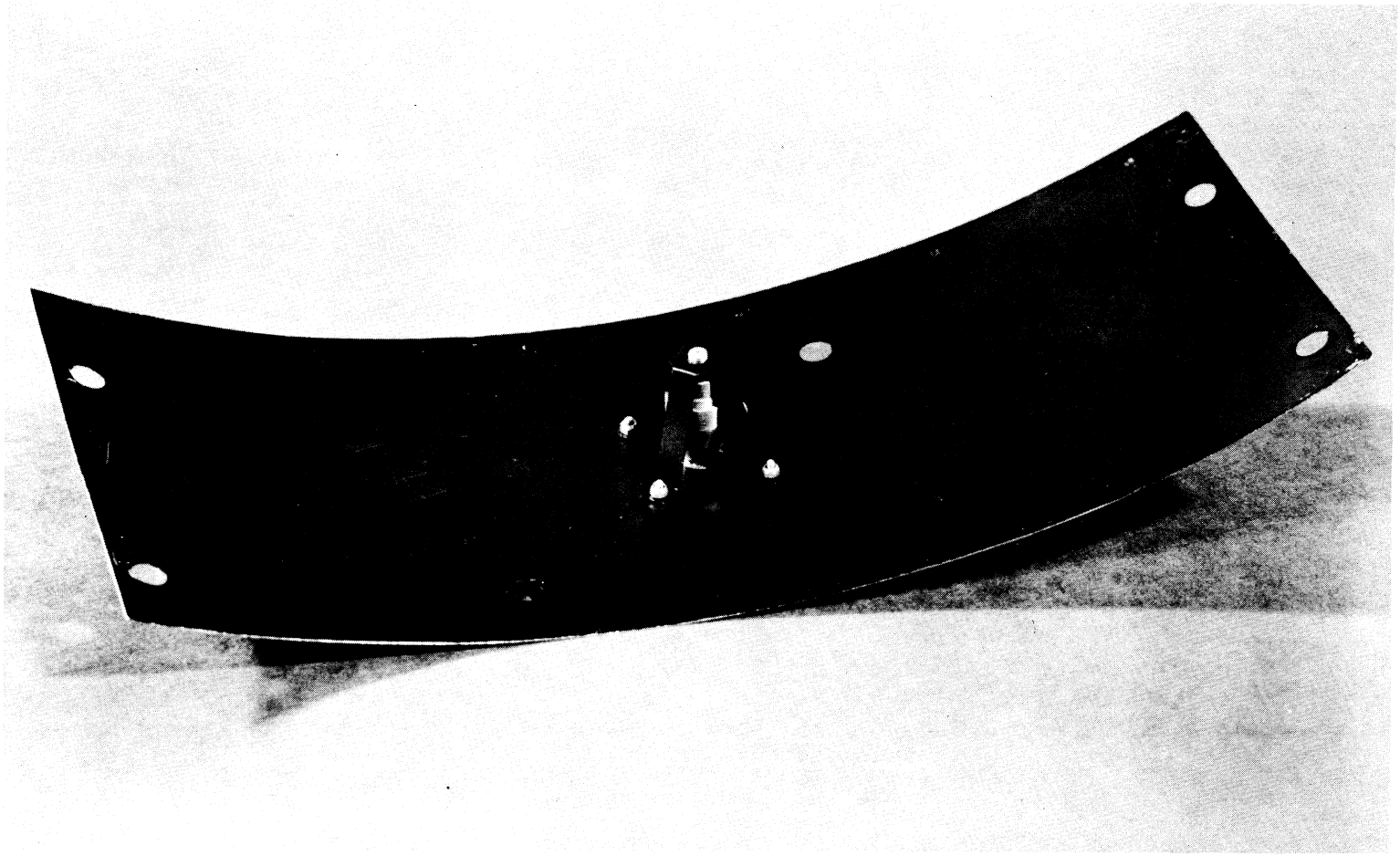

Figure 13. Microphone Assembly for Micrometeorite Detection.

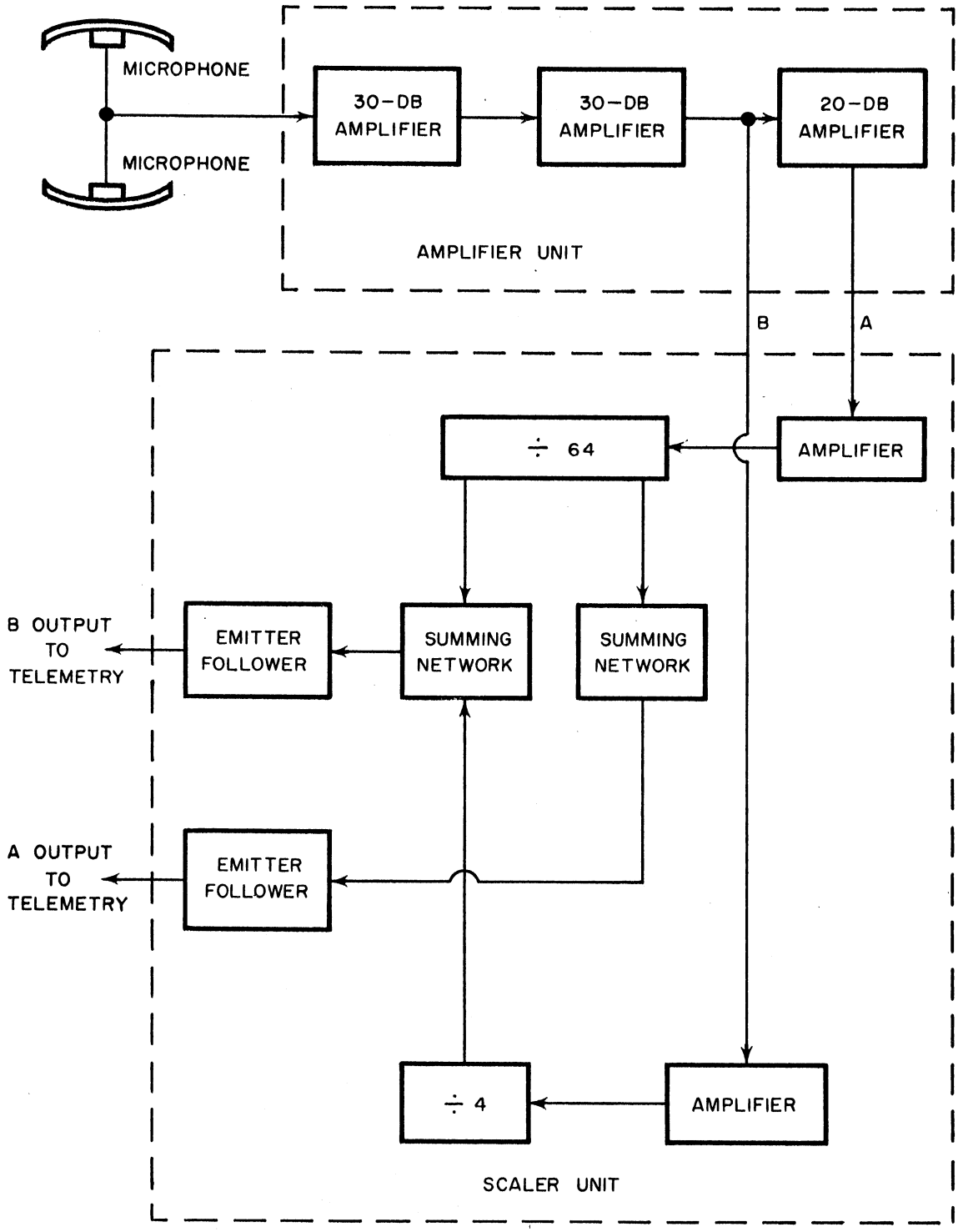

Figure 14. Micrometeorite Detector.

3. INSTRUMENTATION

3.1 Communications

The airborne components of the integrated tracking, telemetry, and command system in Able-5 consist of a command receiver, two 1.5-watt transmitters, the airborne Telebit unit, and two UHF quarter-wave dipole stub antennas, one pair forward for one transmitter, another aft for the second transmitter (see Figure 15). These antenna arrays are made of stainless steel to withstand the heat of the rocket, the forward and aft nozzles of which are between the antenna pairs. The coaxial cable is fabricated from electroless nickel-plated stainless steel components, and the spacers are made of silicon fiberglass to withstand the heat. The radiation pattern for the antennas is omnidirectional; polarization is vertical to the mounting surface. The diplexer is a bandpass device with more than 50-db isolation between transmitter and receiver.

Interrelationships of the payload instrumentation are shown by the functional block diagram of Figure 16.

The payload command receiver (Figure 17) is a transistorized double-conversion, phase-lock-loop unit which produces a coherent output at 2/17 of the received frequency. The receiver operates continuously and, since its 250-cps bandwidth is considerably less than the frequency uncertainty of the received signal, it repeatedly sweeps over a range of 30 kc searching for a carrier, with a sweep period of 30 seconds. When the receiver acquires and locks on a signal from the earth, the sweeping stops and the receiver can then accept any of 20 possible commands. A list of the commands employed in the Able-5 payload is given in Table 3. The receiver has a sensitivity (based on a 12-db noise figure) of about -130 dbm.

Signals from the earth to the payload are transmitted by using a high-power carrier at a frequency of 402 mc, phase-modulated with a 512-cps subcarrier. Amplitude modulation of the subcarrier with a coded train of 13 pulses provides the required information to the digital command system. The receiver weighs four pounds, occupies 1300 cubic inches, and draws 1.5 watts at 16 volts.

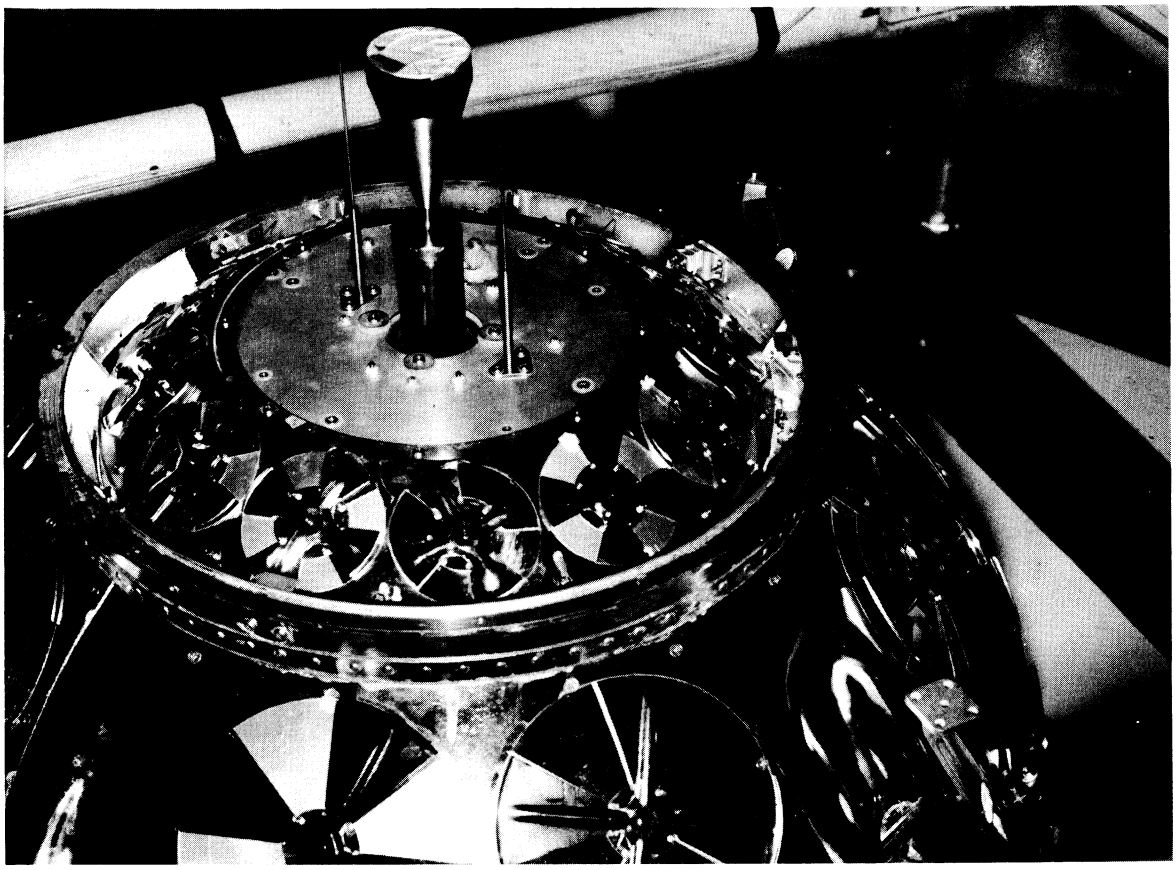

Figure 15. Aft End of Able-5.

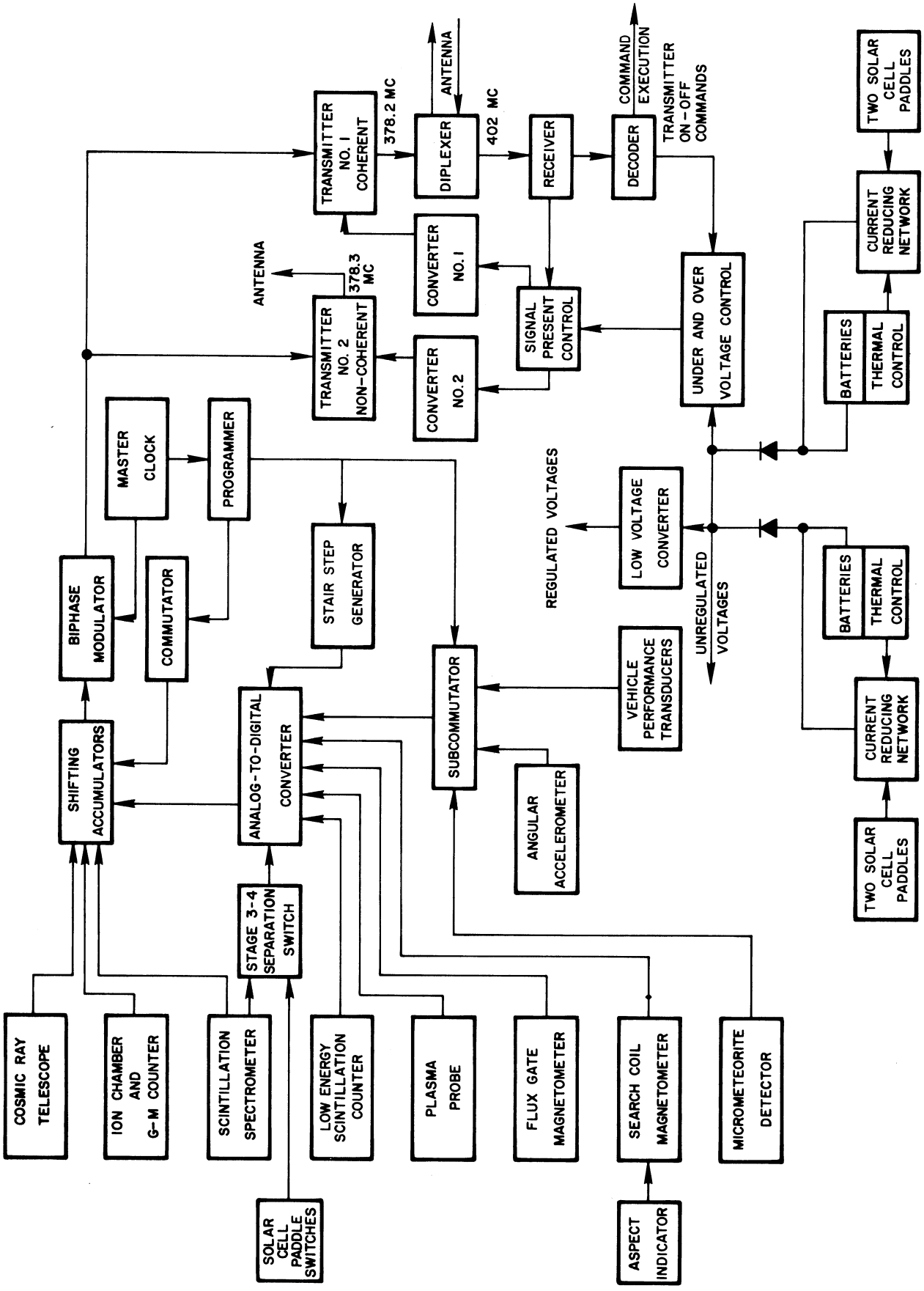

Figure 16. Functional Block Diagram of Able-5.

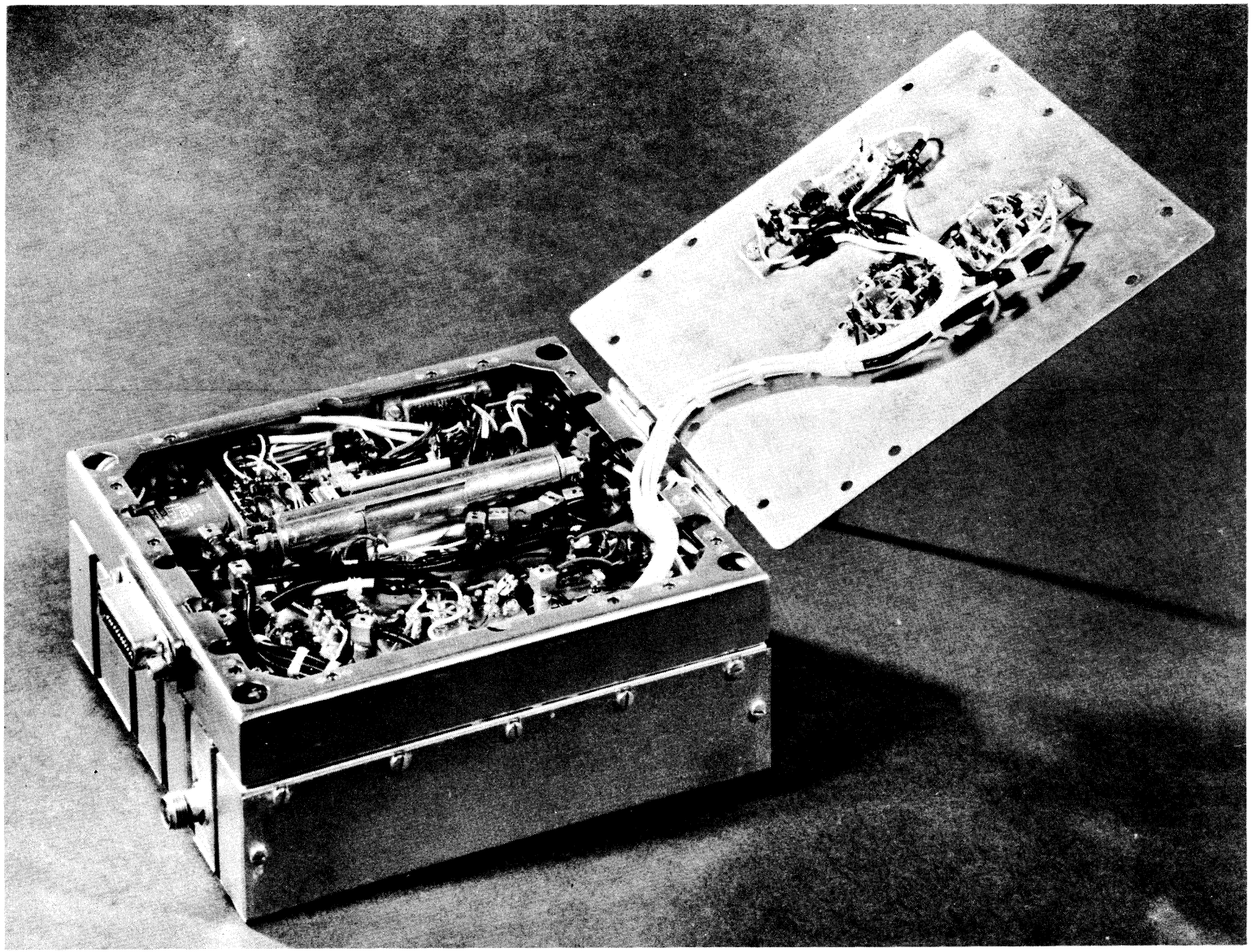

Figure 17. The Able-5 Receiver.

Table 3. Commands to Payload.

1. Telemetry at 64 pps	11. Arm engine No. 5
2. Telemetry at 8 pps	12. Arm engine No. 6
3. Telemetry at 1 pps	13. Start engines
4. Transmitters on	14. Stop engines
5. Transmitters off	15. Arm pressure
6. Clear engines	16. Separate Stages III-IV
7. Arm engine No. 1	17. Flux-gate magnetometer on
8. Arm engine No. 2	18. Scintillation spectrometer on
9. Arm engine No. 3	19. Angular acceleromater on
10. Arm engine No. 4	20. Angular accelerometer off Telemetry subcarrier on

In its role as a transponder, the Able-5 receiver accepts a CW signal from the ground and after suitable processing delivers it to the coherent transmitter at precisely 2/17 of the received frequency. The coherent transmitter accepts the signal from the receiver, multiplies it eight times in frequency, and amplifies it to a 1.5-watt level for retransmission to the ground at about 378 mc. In the process the resultant signal is modulated with a 1024-cps subcarrier containing the time-multiplexed, pulse-code-modulated output of the digital telemetry system. Biphase modulation is employed to impress the telemetry output on the subcarrier.

Range rate is measured on the ground to accuracies of better than 1 ft/sec by extracting the doppler frequency shift between the transmitted and received signal after correcting for the frequency offset introduced by the vehicle transponder. Tracking in angle is performed by nodding the ground antenna alternately in elevation and azimuth. Angular accuracies of about 0.2 degree are possible.

The second payload transmitter, also at 1.5 watts, is operated from its own internal driver, a crystal oscillator. Frequency of this transmitter is offset 100 kc from the nominal transmitted frequency of the coherent transmitter.

Telemetry is impressed on the noncoherent signal in the same manner as on the coherent. The noncoherent transmitter operates from liftoff until Command 20 is sent, which serves to shut off this transmitter. During launch the coherent transmitter filaments are on, but the B+ voltage is not applied until paddle erection. Then the coherent transmitter operates without the telemetry subcarrier until Command 20 is sent. At execution of this command the telemetry subcarrier is applied to the coherent signal, and remains throughout the lifetime of the payload.

Following Command 20, either the coherent or noncoherent transmitter is operated by ground commands. If the payload receiver is locked to a ground carrier signal, the coherent transmitter operates. If the receiver is not locked on to a ground carrier, the noncoherent transmitter operates.

An overvoltage-undervoltage relay is provided which turns off the transmitters if battery voltage drops below 15 volts. The overvoltage control turns on the transmitters if voltage rises sufficiently to insure satisfactory operation, if Command 5 has not been sent.

The digital telemetry unit developed by STL, the Telebit system, is shown being installed in Figure 18. This system accepts both analog and digital inputs from various experiments. The converted information at its output appears as a binary-coded subcarrier (1024 cps), which then phase modulates the transmitters.

The binary output of the Telebit system occurs at a synchronous rate and is composed of repeating sets of frames of words. For Able-5, 11 words per frame are used. One word of each frame is used as a frame sync and is read out as all zeros, while the balance of the words are coded with the digital representation of the input information. Each word contains 12 pulses. The first two pulses (for information words) are always coded the same (zero, one) and define the start of a word; that is, these two pulses provide a word sync. The other 10 pulses take on any combination of binary values to represent a number from 0 to 1023, or divide into subwords of six or four bits. The format for the Able-5 frame is shown in Figure 19. Word 10 of this format subcommutates 21 slowly-varying measurements by means of 16 subcommutated 6-bit words and 9 subcommutated 4-bit words. These measurements are listed in Table 4.

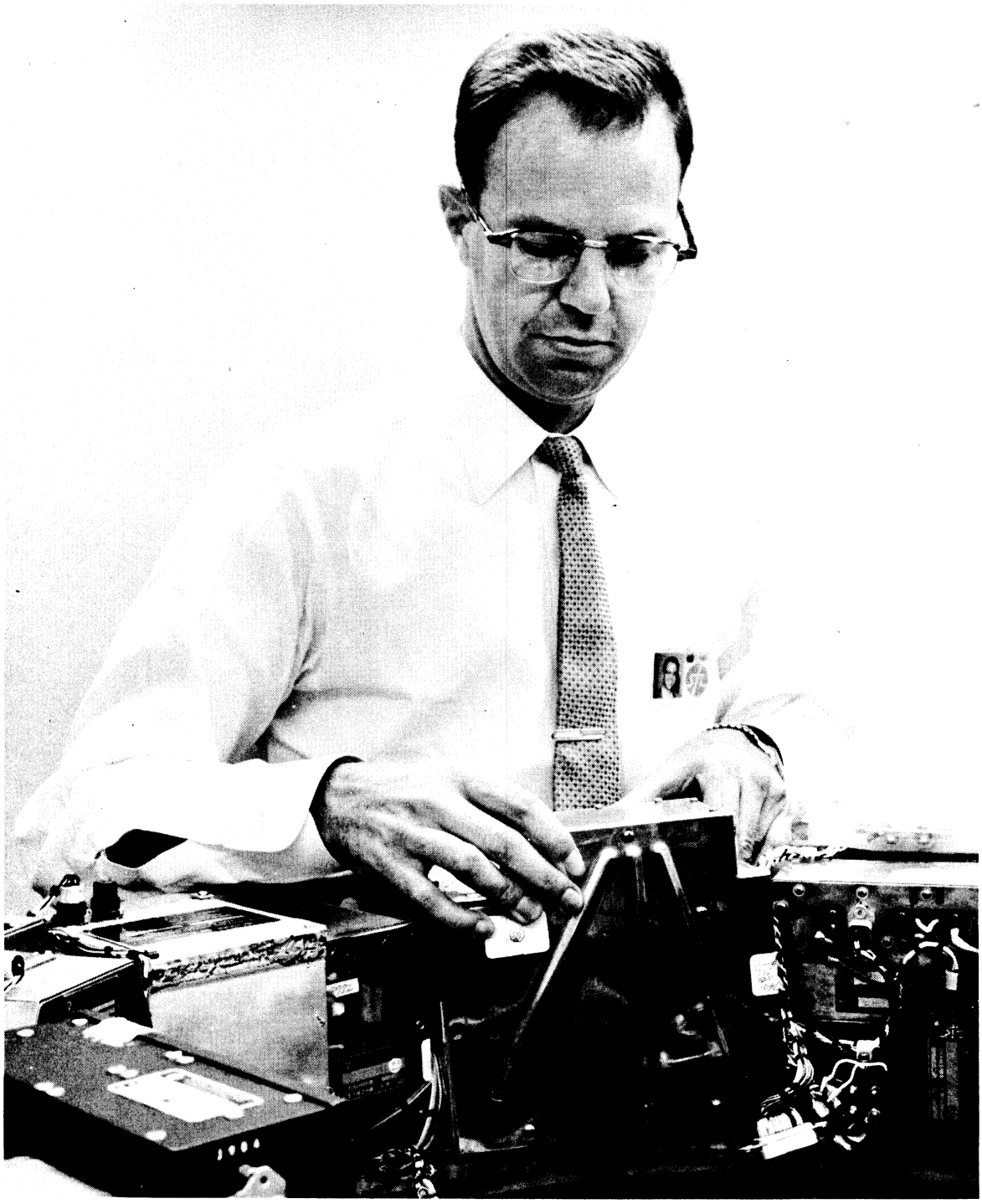

Figure 18. Installation of Telebit in Able-5.

		BIT NUMBER											
MEASUREMENT	WORD NO.	1	2	3	4	5	6	7	8	9	10	11	12
FRAME SYNCHRONIZATION	0	0	0	0	0	0	0	0	0	0	0	0	0
COSMIC RAY TELESCOPE, TRIPLES	1	0	1	32	16	8	4	2	1	8	4	2	1
					HIGH COUNT						LOW COUNT		
COSMIC RAY TELESCOPE, SINGLES	2	0	1	512	256	128	64	32	16	8	4	2	1
SCINTILLATION SPECTROMETER	3	0	1	32	16	8	4	2	1	8	4	2	1
					HIGH COUNT						LOW COUNT		
GEIGER-MUELLER COUNTER	4	0	1	512	256	128	64	32	16	8	4	2	1
IONIZATION CHAMBER	5	0	1	512	256	128	64	32	16	8	4	2	1
LOW ENERGY SCINTILLOMETER *	6	0	1	32	16	8	4	2	1	8	4	2	1
					SCINTILLOMETER						PADDLE OR PULSE HEIGHT		
SPIN COIL MAGNETOMETER	7	0	1	32	16	8	4	2	1	8	4	2	1
					AMPLITUDE						PHASE		
FLUX GATE MAGNETOMETER	8	0	1	32	16	8	4	2	1	8	4	2	1
					DATA						RANGE		
PLASMA PROBE	9	0	1	32	16	8	4	2	1	8	4	2	1
					AVERAGE						PEAK		
SUBCOMMUTATED	10	0	1	32	16	8	4	2	1	8	4	2	1

* THE FOUR-BIT PORTION OF WORD 6 SHOWS ERECTION OF SOLAR CELL PADDLES AT FIRST. AFTER THE PAYLOAD HAS BEEN SEPARATED FROM THE THIRD STAGE, THE BITS SHOW THE PULSE HEIGHT ANALYZER PORTION OF THE SCINTILLATION SPECTROMETER, THE COUNTS FOR WHICH ARE CONTAINED IN WORD 3.

Figure 19. Word Format in Able-5 Telebit.

Table 4. Subcommutated Word Format.

Subcommutated Word	Measurement 6-Bit Portion	Measurement 4-Bit Portion
0	Solar cell current No. 1-2 (1.9 to 0 amp)	Micrometeorite low momentum
1	Solar cell current No. 3-4 (1.9 to 0 amp)	Micrometeorite low and high momentum
2	System voltage (14 to 23 volts)	Angular accelerometer*
3	Transmitter temperature (0 to 150°F)	Identification (3)
4	Converter No. 2 temperature (0 to 150°F)	Combustion chamber firing indicator (on +300 ±50°F, off +200 ±50°F)
5	Battery No. 1-2 temperature (0 to 150°F)	Identification (5)
6	Battery No. 3-4 temperature (0 to 150°F)	Angular accelerometer*
7	DTU temperature (0 to 150°F)	Identification (7)
8	Hydrazine tank pressure (500 to 0 psi)	Lower shelf temperature (0 to 150°F)
9	Receiver loop stress (0 to 3 volts)	Identification (9)
10	Hydrazine temperature (0 to 150°F)	Angular accelerometer*
11	Coating material No. 1 temperature (100 to 430°F)	Identification (11)
12	Upper shelf temperature (0 to 150°F)	Angular accelerometer*
13	Coating material No. 2 temperature (130 to 330°F)	Identification (13)
14	Paddle temperature (-200 to 100°F)	Angular accelerometer*
15	Coating material No. 3 temperature (-150 to 50°F)	Identification (15)

* All zeros when accelerometer is OFF.

A 12-bit combination binary counter and shift register, referred to as a shifting accumulator, is provided in Telebit for each word. Pulses from a digital-type experiment are applied directly to the counting input of a shifting accumulator, while an analog input is applied to an analog-to-digital converter, whose output is then applied to a shifting accumulator. An electronic commutator running synchronously at the word rate, gates 12 shift pulses to each shifting accumulator during one word interval each frame.

These shift pulses cause the information in the shifting accumulator to be delivered to the biphase modulator, and at the same time the output of the digital shifting accumulators is returned to the input so that after 12 shift pulses the state of the shifting accumulators is exactly as it began. The outputs of all of the shifting accumulators are connected together through gates but since only one is shifting at a time no interference results.

The conversion of analog to digital information is done by means of a digital ramp and a voltage comparison circuit. In essence, conversion results from counting the number of steps in the ramp below the level of the analog input voltage. The counting is actually done in a shifting accumulator, just as for digital experiments.

The biphase modulator accepts the pulses emerging sequentially from the shifting accumulators and produces a subcarrier whose phase shifts by 180 degrees each time a binary one is to be transmitted. This biphase-modulated subcarrier is then delivered to the coherent transmitter for phase modulation upon the carrier.

The pulses which cause the electronic commutator to step and the shift registers to shift originate in the programmer, and the programmer in turn receives its excitation from the master clock (see Figure 16). The programmer is equipped such that application of an outside signal derived from the digital command decoder causes the pulse rate of the digital telemetry system to change.

3.2 Power Supply

The Able-5 power supply system is modeled on that designed for the previous Able space probes, Explorer VI and Pioneer V. The system consists of three basic units: solar cells mounted on four extended paddles to convert solar energy to electrical energy, storage batteries, and converters.

The four paddles fold down within the nose fairing of the launch vehicle and at second stage burnout after the fairing has been jettisoned they spring out and latch into place, two extended 22.5 degrees above the payload equatorial plane and two extending 22.5 degrees below. A total of 8800 boron-diffused silicon solar cells are carried on the satellite. Because of attitude and spin considerations, however, only about 2000 of the solar cells are receiving solar energy at one time, and, except for periods of eclipse, this number is relatively independent of payload attitude with respect to the sun.

The payload storage batteries consist of two packs of 14 hermetically sealed, nickel-cadmium cells each, the cells connected in series in each pack and the two packs connected in parallel. Each pack has a nominal output of 18 volts and 3.5 ampere-hour capacity. Part of the power developed in the solar cells is immediately consumed in experiments, the receiver and the transmitter, and the charging rate of the battery is thus lessened by this amount. With a 1.5-watt transmitter operating without solar cell charging current, the batteries can operate for a maximum design time of about four hours. The nominal power available from the solar cells is approximately 30 watts. Two switches are provided in conjunction with these battery packs to prevent the condition of thermal runaway which is likely with nickel-cadmium cells when they are overcharged. These switches open when battery temperature rises above 110°F, thereby removing the charge current until the temperature drops.

The steady-state voltage limit of the batteries is 15 to 21 volts dc. Since this voltage is inadequate for all of the electronics, two sets of static converters are employed to provide a variety of voltage levels. Converter No. 1 provides six output voltages, principally for operation of the experimental sensors, as follows:

Output (volts)	Nominal Load Current (ma)
+6.0 dc	101
-6.0 dc	22
+10.0 dc	270
+16.0 dc	42
-16.0 dc	11
6.0 ac rms	112 rms

Converter No. 2 provides the operating voltages and currents to power the transmitter as follows:

Output (volts)	Nominal Load Current (ma)
+210	30
-20	3
-12	130
+6	10
6.3 ac rms	750

4. HYDRAZINE ROCKET SYSTEM

The monopropellant hydrazine vernier and orbital injection rocket developed by STL for Able-5 is shown in Figure 20. This engine is used to furnish vernier velocity adjustments during the midcourse trajectory of the payload, for which 8300 pound-seconds of impulse and five starts (four aft, one forward) are available. In addition, 26,400 pound-seconds of impulse are available for orbital injection, at the forward nozzle. This retrorocket impulse is provided using the common tankage of the vernier system.

The two thrust chambers are mounted on the spin axis, the vernier chamber facing aft, the injection chamber facing forward. Each nozzle extends approximately eight inches from the payload shell.

Thrust level is nominally 18.5 pounds, varying from 16 to 25 pounds depending on the hydrazine tank pressure. Nozzle expansion ratio is 50:1, and measured specific impulse is 230 seconds.

Both vernier and injection systems are pressure fed. Centrifugal pressure from the spin of the payload forces the propellant to the engine, since the outlet ports for the hydrazine are located along the equator of the hydrazine tank. The vernier system is a decaying-pressure system which uses the gas pressure in the hydrazine tank ullage space for pressurization of the fuel. The injection system employs a regulated pressure system consisting of two spheres containing nitrogen at 2000 psia and a pressure regulator valve set at 250 psia. A normally closed valve is installed on each side of the regulator, and a normally opened valve is fired to close the system. Each of the six possible firings, in fact, requires the use of three explosive-actuated valves, two to start and one to stop the engine. Individual sets of valves are provided for each firing, for a total of 18 valves.

In addition a small four-inch nitrogen sphere pressurized to 2000 psi is utilized after the first vernier firing to provide repressurization of the vernier system.

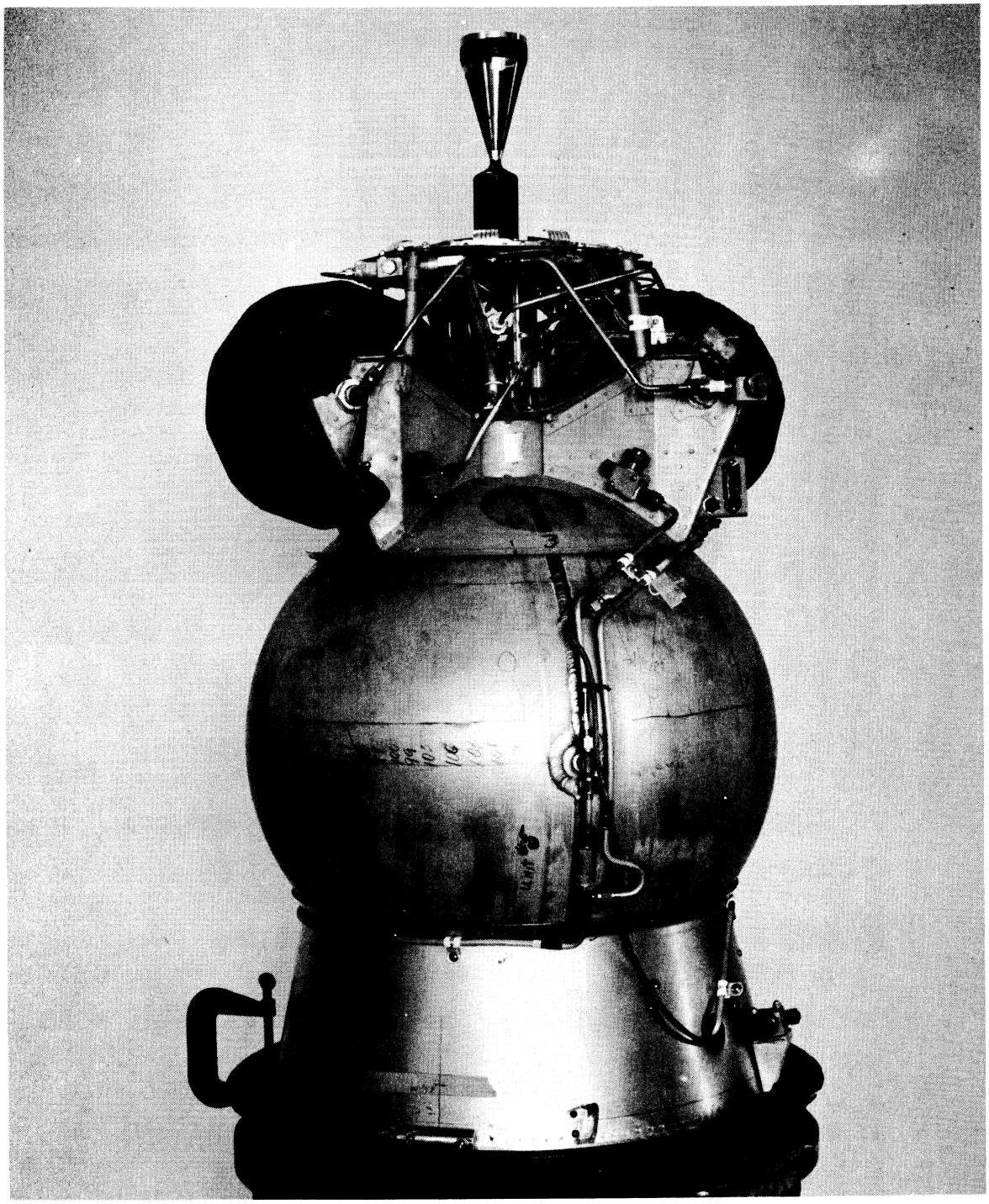

Figure 20. The Able-5 Engine.

The empty engine weighs approximately 57 pounds. Although 178 pounds of hydrazine can be carried, Able-5 carries a total of 151 pounds. Nitrogen gas for pressurization weighs about six pounds, for a total engine weight of 214 pounds.

The sequence of operation for the engine involves four steps.

(1) The normally closed valve in the hydrazine feed line and the normally closed valve in a feed line from eight cubic centimeters of nitrogen tetroxide are fired by command from the ground.

(2) The nitrogen tetroxide, as oxidizer, enters the thrust chamber about 50 milliseconds before the fuel. Since the propellants are hypergolic, chamber pressure rises as soon as the hydrazine enters the chamber.

(3) Oxidizer flow continues for about 200 milliseconds, until the start tank is exhausted. By this time a catalyst, termed H-7, on the walls of the chamber is heated sufficiently to maintain decomposition of the hydrazine.

(4) On command from the ground the normally open explosive valve in the hydrazine line is fired, stopping the flow of fuel and shutting down the engine.

5. TEMPERATURE CONTROL

Optimum performance of Able-5 requires that its internal temperature remain within a range of 40 to 85°F. Three general approaches have been taken to maintain the temperature well within this range. The optimum ratio of absorptivity of sunlight energy to emissivity of heat for the general area of the skin has been carefully calculated, and the polished aluminum appearance of the satellite is the result of this calculation. Radiators are used at those sites in the payload where heat will be generated by operation of the transmitters or converters. And a unique, active temperature control system involving rotating vanes over circles of alternating white and blue has been placed over the skin surface in such a way that the minimum value of controlled area to total area projected from any direction is 36 per cent.

The major function of heat control of the payload is performed by the 50 four-bladed vanes. These vanes are of two sizes, eight-inch and six-inch, to fit onto various locations on the payload. Twelve of the six-inch vanes are grouped about the aft nozzle, 16 eight-inch vanes on the lower shell, and 22 eight-inch vanes on the upper shell.

These vanes are attached through bimetallic springs to the payload skin. Figure 21 shows the vanes being attached to the payload on the launch stand. The tension of the spring is sensitive to the temperature at its location and dictates the angle at which the vanes stand. At one extreme, about 75°F, a vane completely exposes the white areas; at the other extreme, about 50°F, the vanes have moved through 45 degrees to expose the blue areas completely. A portion of the payload shell is shown in Figure 22; the lower portion of the figure shows the vanes at high temperature, the upper portion at low temperature.

Since silicon solar cells suffer a loss of efficiency with increased temperature, the paddles must remain colder than the body of the satellite, and thus the temperature control of the paddles is a separate problem. The paddles are thermally insulated from the shell, but each paddle is thermally coupled fore and aft so that heat radiation from the side of the paddle in shadow will be approximately equal to the side in sunlight. A thin glass plate, 0.003-inch thick,

Figure 21. Attachment of Temperature-Control Vanes to Payload.

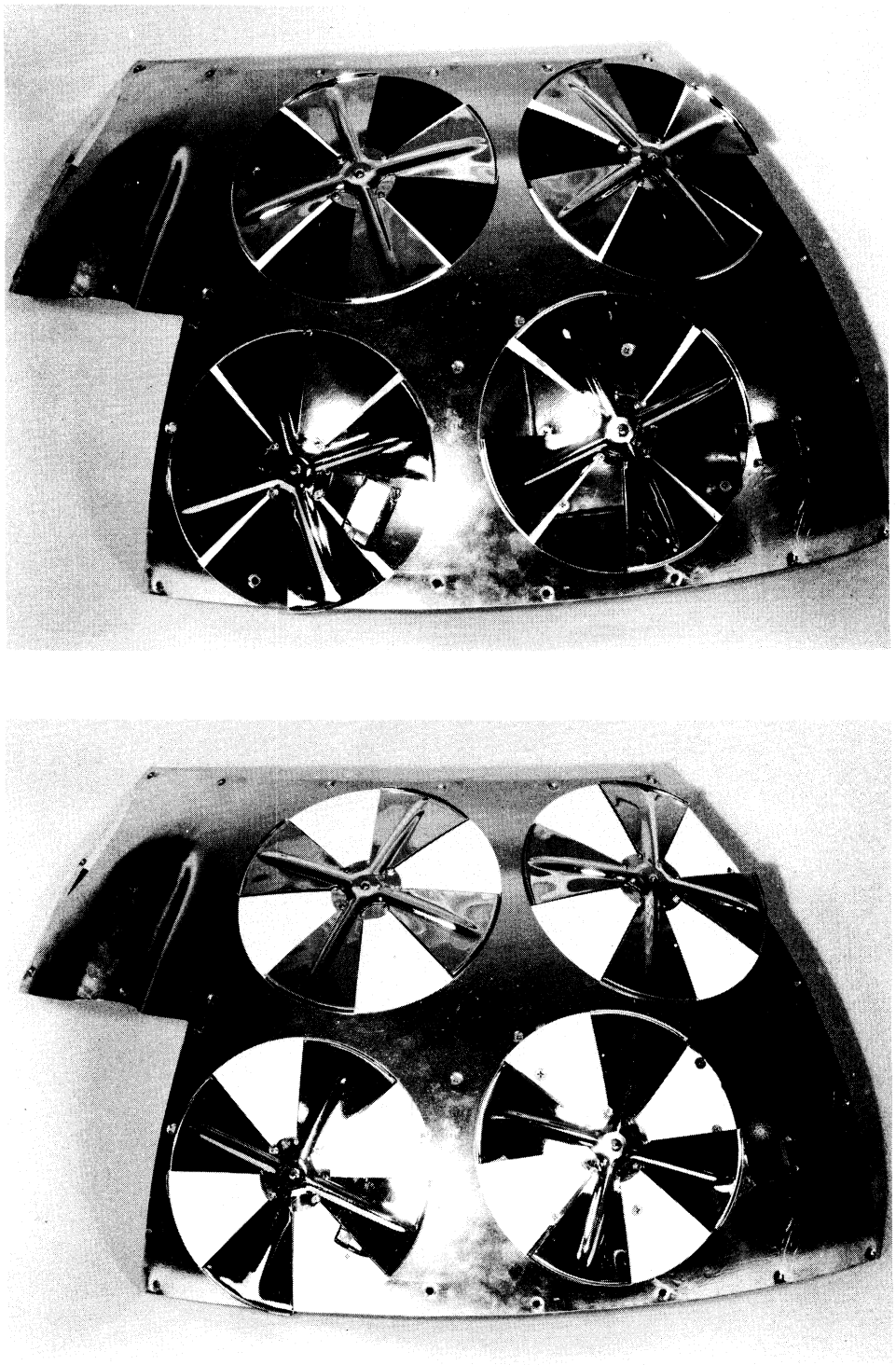

Figure 22. Temperature Control Vanes on Able-5 Shell.

with an interference filter vacuum deposited on the under side, is cemented onto each cell. The infrared filter serves to reject all solar energy below 0.49 micron in the spectrum, which has little effect on the power response of the cell but eliminates a significant portion of the heat response of the cell. By this means the temperature of the solar cell paddles is expected to remain about 5°F, which is close to optimum for the cells.

As an adjunct to the temperature control system an experiment is carried on Able-5 to test the effects of the space environment on three coatings. Three one-inch aluminum spheres jutting from the payload near the equator are each covered with a thin coating of, respectively, a relatively high heat absorptance, a relatively high heat emittance, and a combination of relative low values of both of these properties. Temperature sensors in each of these spheres, the first in the range 100 to 430°F, the second -150 to 50°F, and the third 130 to 330°F, provide a measurement of the changing properties of the materials while they are exposed to the space environment.